Organic & Biomolecular Chemistry

PAPER

View Article Online
View Journal | View Issue

Cite this: *Org. Biomol. Chem.*, 2018, **16**, 8769

Potent anti-proliferative activities of organochalcogenocyanates towards breast cancer†

Kaustav Banerjee,[a] Ganesan Padmavathi,[b] Debojit Bhattacherjee,[a,c] Suchismita Saha,[a] Ajaikumar B. Kunnumakkara[b] and Krishna P. Bhabak *[a,c]

Received 3rd August 2018,
Accepted 30th October 2018

DOI: 10.1039/c8ob01891j

rsc.li/obc

The pharmacological importance, particularly the anti-cancer and chemopreventive potentials, of organochalcogen compounds has attracted wide research attention recently. Herein we describe the synthesis of a series of organochalcogenocyanates that have one or more selenocyanate or thiocyanate units in a single molecule. The anti-proliferative activity of these organochalcogenocyanates in different breast cancer cells shows that selenocyanates exhibit much higher anti-proliferative activities than thiocyanates in general. Our study reveals that the activity of benzyl selenocyanate (**1**, BSC) could be significantly enhanced by 4-nitro substitution (**12**), which was more selective towards triple-negative breast cancer cells (MDA-MB-231) over other ER+ breast cancer cells (MCF-7 and T-47D). Furthermore, to the best of our knowledge, this is the first report on the synthesis of compounds having more than two selenocyanate units with promising anti-proliferative activities. Our studies further indicate that the apoptotic activities of selenocyanates are associated with modulation of cellular morphology and cell cycle arrest at S-phase. Selenocyanates also inhibited cellular migration and exhibited weak antioxidant activities. An effective binding interaction of compound **12** with serum albumin indicates its feasible transport in the bloodstream for its enhanced anti-cancer properties. Mechanistic studies by western blot analysis demonstrate that benzylic selenocyanates exhibit anti-proliferative activities by modulating key cellular proteins such as Survivin, Bcl-2 and COX-2; this was further supported by molecular docking studies. The results of this study would be helpful in designing suitable chemotherapeutic and chemopreventive drugs in the future.

Introduction

Cancer, characterized by uncontrolled cell proliferation, is one of the major and leading causes of mortality throughout the world.[1] Among different organ-specific cancers, breast cancer has become a very common disease and is the second leading cause of mortality among women worldwide.[1] Although chemotherapy is the widely used traditional strategy for preventing or treating cancer, this treatment becomes inefficient in many cases for one or more reasons such as (i) the lack of selectivity of most of the chemotherapeutic drugs, (ii) increased resistance of cancer cells towards the drugs and (iii) additional toxicities. Particularly, the treatment scope of breast cancer in an advanced stage is very much limited due to its high resistance to traditional treatments such as chemotherapy.[2] While the hormonal treatment of the estrogen receptor positive (ER+) breast cancer is accompanied by undesired side effects, there is no effective treatment to date for estrogen receptor negative (ER−) breast cancer, especially the triple-negative sub-types, and thus the patients suffer from very poor prognoses.[3] Therefore it is very important and necessary to identify suitable therapeutic compounds for breast cancer, which would suppress the growth of ER− breast cancer cells as well as minimize the undesired side effects.

Very recently Giles and co-workers have reported a very simple organoselenium compound, diphenyl diselenide (DPDS), which exhibits significantly higher cytotoxicity towards triple-negative breast cancer (TNBC) cells over other breast cancer cells.[4] It has been described in several studies that the treatment of cancer by chemotherapeutic drugs such as cisplatin, cyclophosphamide, doxorubicin *etc.* is associated with significant side-effects and toxicities mainly due to an

[a]*Department of Chemistry, Indian Institute of Technology Guwahati, Guwahati-781039, Assam, India. E-mail: kbhabak@iitg.ac.in; Fax: +91-361-258-2349; Tel: +91-361-258-3476*
[b]*Cancer Biology Laboratory & DBT-AIST International Laboratory for Advanced Biomedicine (DAILAB), Department of Biosciences and Bioengineering, Indian Institute of Technology Guwahati, Guwahati-781039, Assam, India*
[c]*Centre for the Environment, Indian Institute of Technology Guwahati, Guwahati-781039, Assam, India*

†Electronic supplementary information (ESI) available. See DOI: 10.1039/c8ob01891j

overproduction of reactive oxygen species (ROS) or reactive nitrogen species (RNS).[5] An efficient strategy for minimizing these toxicities is developed by combination therapy utilizing the chemopreventive approach in the presence of suitable antioxidants or pro-antioxidants. It has been shown that natural and/or synthetic organoselenium compounds are suitable candidates for chemoprevention and would dramatically minimize chemotherapeutic drug-induced toxicities as well as enhance their potencies.[6] The chemopreventive activities of inorganic and organic selenium compounds on multiple mammary tumor model systems such as chemically induced mammary carcinogenesis in rats/mice as well as spontaneous tumorigenesis in mice have been reported earlier.[7] These studies clearly demonstrated that organoselenium compounds are much more potent than the corresponding organosulfur compounds and inorganic selenium species.[8] In 1995, El-Bayoumy and co-workers showed that a simple organoselenium compound, benzyl selenocyanate (**1**, BSC), effectively inhibits DMBA-induced mammary tumors in rats during the initiation phase of carcinogenesis; however, its sulfur analogue benzyl thiocyanate (**2**, BTC) and sodium selenite (Na_2SeO_3) had no effect (Fig. 1).[9] Subsequently, in 1997, Reddy *et al.* reported the chemopreventive ability of two synthetic organoselenium compounds, namely 1,4-phenylenebis(methylene) selenocyanate (**3**, *p*-XSC) and *p*-methoxybenzyl selenocyanate (**6**), towards colon carcinogenesis in rats that were treated with the carcinogen azoxymethane and fed low- or high-fat diets (Fig. 1).[10] Dietary administration of these drugs during the initiation and post-initiation periods inhibited colon tumor incidence in rats maintained on a high-fat diet. The chemopreventive action of compound **3** was found to be more pronounced when it was administered along with a low-fat diet. The metabolic pathway of compound **3** was studied further and it was found that the selenocyanate moiety reacted with the cellular abundant glutathione (GSH) with the replacement of the cyano group leading to the formation of the corresponding selenenyl sulfide compound **5**. The chemopreventive activity of **5** was also evaluated and found to be almost equal to that of compound **3**. Detailed studies by Bhattacharya and co-workers have established that diphenylmethyl selenocyanate (**7**) has the ability to counter the oxidative stress induced by xenobiotics of diverse nature *in vivo*.[11] They have also developed a series of naphthalimide-based selenocyanates that were found to be very effective towards the cyclophosphamide (CP)-induced genotoxicity and oxidative stress.[12] These compounds protect against chemotherapeutic drug-induced toxicity *in vivo* and chemoprevention can be initiated without blocking the antitumor effects of chemotherapeutic drugs.[13] Dong and co-workers have reported an interesting observation that a second generation organoselenium compound, methylseleninic acid ($MeSeO_2H$), significantly enhanced the anti-cancer potency of paclitaxel towards TNBC cells (MDA-MB-231).[14] Although different organoselenium compounds such as monoselenides, diselenides, selenoesters, and cyclic selenenyl amides have been reported to exhibit significant anti-proliferative activities towards different organ-specific cancer cells, reports on the anti-proliferative activities of organoselenocyanates and the corresponding thiocyanates are relatively rare.[15] Very recently, Sharma and co-workers have reported the anti-cancer activity of a novel non-steroidal anti-inflammatory drug (NSAID)-based selenocyanate (**8**) towards a series of cancer cells.[16] The compound was found to be specific towards colorectal cancer (CRC) cells and inhibited their growth by arresting the cell cycle at G1 and G2/M phases. Attention towards TNBC cells was further enhanced by the recent report on benzimidazole-based selenadiazole compounds **9–11**, which exhibit excellent anti-proliferative activities towards MDA-MB-231 cells over MCF-7 cells.[17] From various studies it has been elucidated that the metabolic pathways of organoselenium compounds followed by the relative toxicities of major metabolic products are crucial for their chemopreventive activities.[18] A possible metabolic pathway of organoselenocyanates such as *p*-XSC indicates its feasible reaction with intracellular glutathione (GSH) to generate the corresponding glutathione adduct.[19] Therefore, before considering organoselenocyanates as chemopreventive agents in combination or adjuvant therapies, it is very important to understand their anti-proliferative activities.

Inspired by the enhanced chemopreventive efficacies of *p*-XSC (**3**) as compared to BSC (**1**), we attempted to synthesise a series of benzylic and mesitylenic selenocyanates that have one or more selenocyanate moieties in a single molecule with the intention of exploring their efficacy as potential anti-proliferative agents. To understand the importance of selenium or selenocyanate groups in these compounds, the corresponding thiocyanates were also synthesized for a detailed structure–activity correlation study under identical test conditions. As the breast cancer expressing estrogen receptor (ER) and progesterone receptor (PR) have a better prognosis than triple-negative breast cancers, our test compounds were screened first for their anti-proliferative activities *in vitro* towards the triple-negative cell line MDA-MB-231. Furthermore, the potent compounds were subsequently screened in other ER+ breast cancer cells such as MCF-7 and T-47D to gain further comparative results on breast cancer cells in general. The most potent compound was studied further to understand its mode of action towards anti-proliferative activities (Fig. 2).

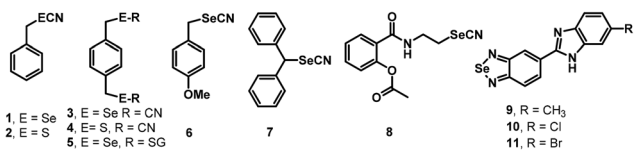

Fig. 1 Chemical structures of some organochalcogen-based chemopreventive agents **1–11**.

Results and discussion

Synthesis of chalcogenocyanates

We present herein the synthesis of benzylic and mesitylenic poly-substituted selenocyanates and the corresponding thio-

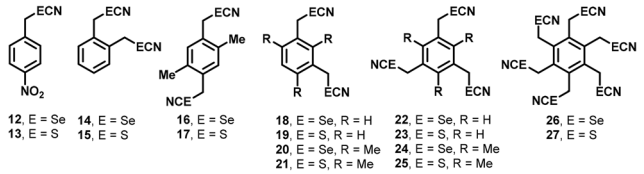

Fig. 2 Chemical structures of benzylic and mesitylenic poly-selenocyanates and the corresponding poly-thiocyanate analogues.

cyanates **12–27**. These compounds were conventionally prepared in good yields by nucleophilic substitution reactions from the corresponding halides. The selenocyanates in the present study were prepared from the corresponding halides in the presence of potassium selenocyanate (KSeCN) as a nucleophile following the literature method with minor modifications.[20] The thiocyanate counterparts were synthesized from the same halides in the presence of potassium thiocyanate (KSCN) in dry methanol under reflux conditions following the earlier reported method with minor modifications.[21] The commercially unavailable precursor halides were synthesized in the laboratory in one or two steps wherever applicable (ESI†). The final selenocyanates and thiocyanates were purified by column chromatography and characterized by NMR, IR and ESI-MS analyses (ESI†).

Anti-proliferative activity of chalcogenocyanates in breast cancer cells

As discussed earlier that the treatment scope for triple-negative breast cancer is limited and not well established, we have chosen MDA-MB-231 cells to understand the efficacy of our synthesized compounds. The anti-proliferative activity of these compounds was evaluated using MTT assay in MDA-MB-231 cells. All the experiments were independently carried out at least three times and the results were summarized after 72 h of incubation at 37 °C. To understand the dose-dependency of these compounds for growth inhibition of MDA-MB-231 cells over 72 h, the percentage of cell proliferation was estimated at four different concentrations (1.0 μM, 5.0 μM, 10.0 μM and 25.0 μM) and compared to that in the absence of compounds (controls) as well as with a well-known anti-cancer drug, 5-fluorouracil (5-FU). As shown in Fig. 3, most of the organo-selenocyanates were found to be active in the growth inhibition of MDA-MB-231 cells but the corresponding thiocyanate analogues were found to be almost inactive under identical experimental conditions. A decreased rate of proliferation was observed with an increase in concentration up to 10.0 μM and a noticeable cytotoxicity (negative % proliferation) was detected for almost all the selenocyanates at 25.0 μM concentration. A strong inhibition was observed for compound **12** even at 1.0 μM concentration and cytotoxic behaviour was detected at concentrations 10.0 and 25.0 μM. This could be indicative of the very high potency of compound **12** as compared to other derivatives. Whereas moderate inhibition and no cytotoxicity was observed for compounds **1**, **14**, **22** and **26** up to 25.0 μM concentration, indicating relatively weaker

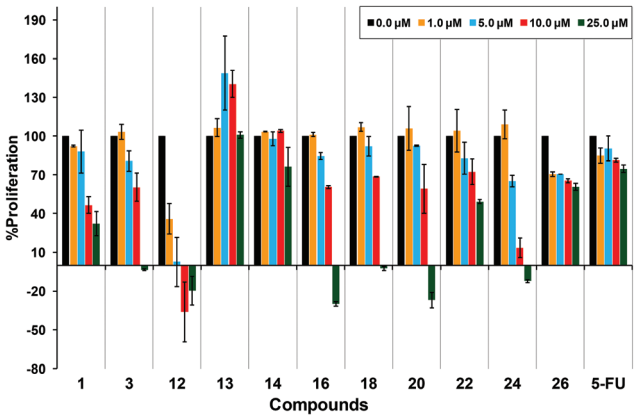

Fig. 3 Percentage proliferation of MDA-MB-231 cells by the test compounds in a dose-dependent manner. In addition to control experiments, % proliferation was studied at four different concentrations (1.0 μM, 5.0 μM, 10.0 μM and 25.0 μM). The % proliferation after 72 h as shown above was calculated from the resultant OD values at 72 h after subtracting the OD values of an identical set of cells at 0 h. Therefore, the negative % proliferation values at some compound concentrations indicate the presence of a smaller number of live cells at 72 h than that at 0 h (cytotoxicity).

growth inhibitory activities. Interestingly, most of the organo-selenocyanates exhibited better efficacy than the standard anti-cancer drug 5-FU under identical experimental conditions in MDA-MB-231 cells.

After determining the dose-dependency of the test compounds towards growth inhibition of MDA-MB-231 cells, inhibitory concentrations towards cell proliferation were determined for the potent compounds to understand their relative anti-proliferative activities (Table 1). Standard and previously reported chemopreventive selenocyanate compounds such as benzyl selenocyanate (BSC, **1**) and *p*-XSC (**3**) exhibited good anti-proliferative activities with an IC_{50} of 11.15 and 12.13 μM, respectively. Interestingly, compound **12** having 4-NO_2 substitution at the phenyl ring exhibited very high potency (IC_{50} = 0.80 μM), which was almost 14-fold and 15-fold more potent than standard selenocyanates **1** and **3**, respectively. Similar to *p*-XSC, other bis-selenocyanates such as **16**, **18** and **20** exhibi-

Table 1 IC_{50} values of some active selenocyanates for their anti-proliferative activities in MDA-MB-231 cells as determined by MTT assay

Compound	IC_{50} [a] value (μM)	Compound	IC_{50} [a] value (μM)
1	11.15 ± 2.75	**18**	13.90 ± 0.12
3	12.13 ± 2.19	**20**	11.66 ± 2.61
12	0.80 ± 0.14	**24**	6.43 ± 0.10
16	11.73 ± 0.23		

[a] Data represent the mean IC_{50} values (±SD) of % cell proliferation determined by the MTT assay from the dose–response curves in triplicate after 72 h of incubation at 37 °C. About 4000 cells per 100 μl per well were seeded in 96-well culture plates and treated with various concentrations of test compounds for 72 h. The % proliferation after 72 h as shown above are calculated from the resultant OD values at 72 h after subtracting the OD values of an identical set of cells at 0 h.

ted comparable IC_{50} values in the range of 11–14 μM as shown in Table 1. However, the corresponding *ortho*-derivative **14** was found to have weaker anti-proliferative activity and its IC_{50} could not be determined in a similar concentration range. A significant difference in anti-proliferative activity was observed between compounds **22** and **24** having three selenocyanate units. While an IC_{50} value could not be determined for compound **22** up to a concentration of 25 μM, the corresponding mesitylenic derivative **24** exhibited a significantly improved anti-proliferative activity (IC_{50} = 6.43 μM). These results indicate that the presence of the methyl group in benzylic selenocyanates might play important roles in their anti-proliferative activities, which is clearly reflected in the activities of compounds having two (**14**, **16**, **18** and **20**) and three (**22** and **24**) selenocyanate units. However, to our surprise, the IC_{50} value could not be determined in the MTT assay for compound **26** with six selenocyanate units. A decrease in cell proliferation was observed in the beginning with increasing concentration of compound **26**; however, negligible change was observed after 40% inhibition. This is also reflected in the dose–response data as shown in Fig. 3. Due to the presence of six selenocyanate units in a single molecule, compound **26** became very lipophilic in nature and was sparingly soluble in the buffered medium during cellular assays. Therefore, accurate inhibitory activity could not be determined at higher concentrations. As thiocyanates were almost inactive up to 25 μM concentration, IC_{50} values were not determined for these compounds and the inhibitory responses of some representative thiocyanates are shown in the ESI.† As observed in Fig. 3 and Table 1, it is evident that the anti-proliferative activity of benzyl selenocyanate **1** can be dramatically enhanced by a simple substitution of a nitro group at the 4-position (compound **12**) or by a proper balance of methyl and selenocyanato groups in a single molecule (compound **24**).

After screening all the selenocyanates and some representative thiocyanates in triple-negative breast cancer cells (MDA-MB-231), we further screened some of the active compounds (**1**, **12** and **24**) along with the standard drug 5-FU in two additional ER+ breast cancer cells (MCF-7 and T-47D) to understand the impact of these compounds on breast cancer cells. As shown in Fig. 4, the compounds were found to be potent in both the cell lines. While the activities of these selected compounds in both of these ER+ breast cancer cells were almost comparable, the activities were significantly different as compared to MDA-MB-231 cells. For example, although compound **12** (IC_{50} = 0.80 ± 0.14 μM) was significantly more active than compound **24** (IC_{50} = 6.43 ± 0.10 μM) in MDA-MB-231 cells, a reversal in potency was observed in both MCF-7 and T-47D cells. In these cells, compound **12** [IC_{50} (MCF-7) = 7.71 ± 0.45 μM; IC_{50} (T-47D) = 13.17 ± 3.6 μM] was found to be less active than compound **24** [IC_{50} (MCF-7) = 4.64 ± 0.13 μM; IC_{50} (T-47D) = 3.53 ± 0.74 μM]. These results indicate that although compound **24** is moderately active on all three breast cancer cells studied herein, selenocyanate **12** is highly selective towards triple-negative breast cancer cells (MDA-MB-231) over other ER+ breast cancer cells (MCF-7 as well as T-47D).

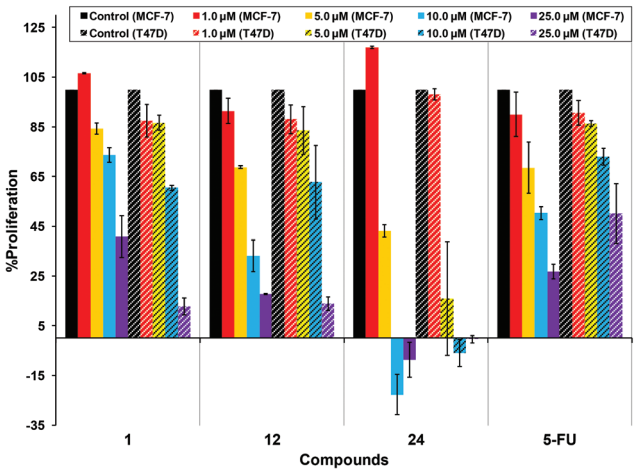

Fig. 4 Percentage proliferation of MCF-7 and T-47D cells in the presence of some selected test compounds in a dose-dependent manner. In addition to control experiments, % proliferation was studied at four different concentrations (1.0 μM, 5.0 μM, 10.0 μM and 25.0 μM). The % proliferation after 72 h as shown above was calculated from the resultant OD values at 72 h after subtracting the OD values of an identical set of cells at 0 h. Therefore, the negative % proliferation values at some compound concentrations indicate the presence of a smaller number of live cells at 72 h than that at 0 h (cytotoxicity).

To understand the selectivity of the most active compound **12** towards a cancer cell over normal cells it was screened further in a representative normal cell line, L-132 (human lung embryonic epithelial cells), and the results were compared to that of MDA-MB-231 cells. As the IC_{50} of compound **12** in MDA-MB-231 cells was around 1.0 μM, the anti-proliferative activity was checked at 1.0 μM and at 5-fold higher concentration (5.0 μM). As expected, the anti-proliferative activity was found to be much weaker in L-132 cells at both the concentrations (Fig. S24, ESI†), indicating significant selectivity of compound **12** towards triple-negative breast cancer cells over normal cells.

Dose dependent cellular death study by a PI-flow cytometric assay

As seen in Fig. 3, some of the selenocyanates exhibited cytotoxic behavior at higher concentrations; this was further confirmed using a propidium iodide (PI)-flow cytometric assay. PI is a fluorescent compound that can bind to nucleic acids with little or no sequence preference. An increased red fluorescence is indicative of a damaged cell membrane, which in turn represents cell death. Among the test compounds used in this study, five selenocyanates, namely, **3**, **12**, **18**, **20** and **24**, that exhibited cytotoxic behavior were chosen for the PI-flow cytometric assay. Treatment of MDA-MB-231 cells with different concentrations of these test compounds for a duration of 72 h resulted in profound cell death, which was found to be dose-dependent as shown in Fig. 5. At the concentrations of 10 and 25 μM of selenocyanates, significant cell death was observed,

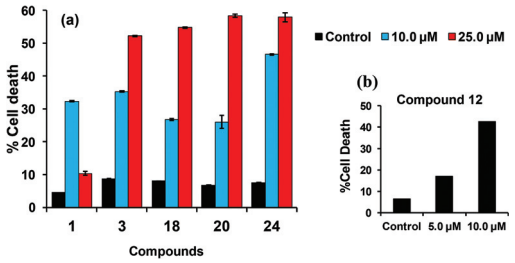

Fig. 5 Cytotoxicity profiles of the test compounds on MDA-MB-231 cells in propidium iodide (PI)-flow cytometric studies. About 5 × 10^4 cells per 2 mL were seeded in 6-well culture plates and treated with two different concentrations (10 μM and 25 μM) of test compounds for 72 h. A concentration of 5.0 and 10.0 μM was used only for compound **12**. The cells were stained with 5.0 μl of 1.0 mg mL^{-1} of PI and analyzed by the flow-cytometric method.

which is in agreement with the observation from the anti-proliferative activity data obtained from the MTT method. As the IC_{50} of compound **12** was much lower, relatively lower concentrations (5 and 10 μM) were used and around 40% cell death was observed at 10 μM concentration. This study along with anti-proliferative activity data confirms the inhibition of cell growth and induction of cell death by the organoselenocyanates used in the present study.

Cell cycle progression analysis of MDA-MB-231 cells in the presence of selenocyanates

A proper regulation of the cell cycle is an essential process for normal cell development and cellular functions. A de-regulation of it may induce aberrant cell proliferation, leading to cancer. Therefore, an inhibition of abnormal cell cycle progression, which would result in reduced cell proliferation and increased apoptosis, is one of the main strategies for cancer therapy. In the present study, in order to understand the mechanism of inhibition of cell proliferation by the test compounds, we have investigated the effects of some active selenocyanates such as **12** and **24** on the cell cycle distribution of MDA-MB-231 cells using PI-based flow-cytometric experiments. Cell cycle distribution was observed upon the incubation of cells with test compounds for 24 h at two different concentrations, namely 1.0 μM and 5.0 μM. As shown in Fig. 6, a noticeable arrest in cell cycle progression was observed in the presence of compounds **12** and **24**. These results show that the test compounds effectively increase the population at S-phase in a dose-dependent manner with a concomitant decrease in population in G1 and G2 phases. For example, S-phase population is increased to 38.8% (1.0 μM) and 57.9% (5.0 μM) from 33.3% (control) in the presence of compound **12**. These results indicate that the pronounced anti-proliferative activity of compound **12** as reflected in apoptotic assays is probably through the induction of cell cycle arrest in S-phase. Similarly, compound **24** having three selenocyanate units also exhibited reasonable cell cycle arrest in S-phase, indicating a similar mode of action towards their anti-proliferative activities. The influence of selenocyanates on the cell cycle distribution of

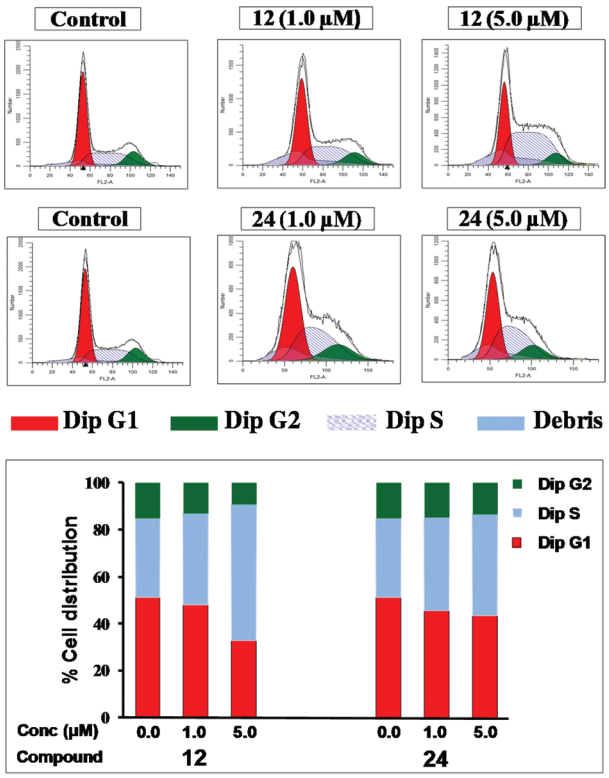

Fig. 6 Graphical representation of distribution patterns of MDA-MB-231 cells in different phases of cell cycle in the presence of selenocyanates **12** and **24**. About 1 × 10^5 cells per 2 mL were seeded in 6-well plates and treated with two different concentrations (1.0 and 5.0 μM) of test compounds for 24 h and the cell cycle distribution was analyzed by flow-cytometric assay after staining with PI/RNase.

MDA-MB-231 cells observed in the present study is in contrast to the effect of selenadiazole derivatives **9–11** on MDA-MB-231 cells.[17]

Compounds **9–11** induced an effective increase of cell population in Sub-G1 and G2/M phases leading to early and late apoptosis. However, a similar S-phase arrest has been reported in MCF-7 cells in the presence of an aromatic organoselenium compound such as bis(4-aminophenyl) diselenide.[22]

Inhibition of the migration of cancer cells

In addition to primary cancer cells, metastatic cells mainly spread the cancer to other parts of the body. As the metastasis takes place due to cell migration, inhibition of cancer cell migration is very important for the therapeutic process. Furthermore, a high rate of metastasis is observed for the TNBC cells and there are a limited number of drugs known to have significant anti-migratory properties towards TNBC cells. We have therefore evaluated some selected selenocyanates for their anti-migratory properties towards MDA-MB-231 cells using a wound healing assay.[23] Regular monitoring of the cells revealed that the compounds inhibited the migration of the cells to the wounded area, indicating the anti-invasive nature of test compounds (Fig. 7). For example, significant dose-

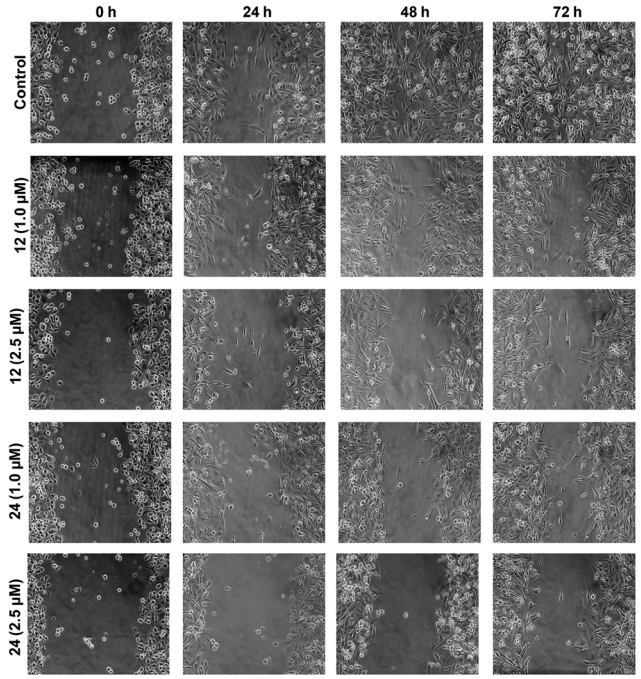

Fig. 7 Wound healing studies on MDA-MB-231 cells in the presence of compounds **12** and **24** at a concentration of 1.0 μM and 2.5 μM after incubation for 0 h, 24 h, 48 h and 72 h.

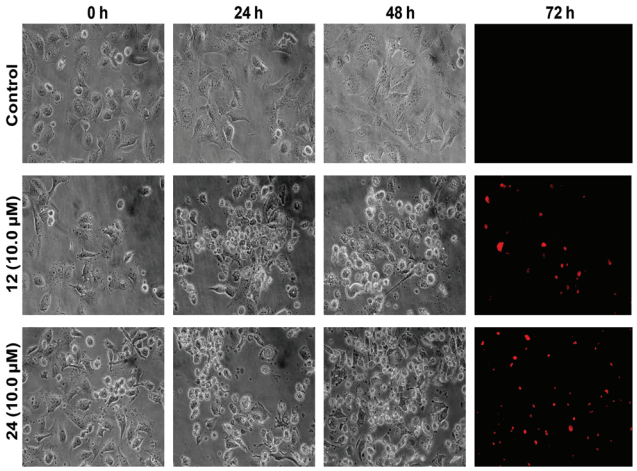

Fig. 8 Change in cellular morphology of MDA-MB-231 cells in the absence and presence of selenocyanates **12** and **24** at a concentration of 10.0 μM after incubation for 0 h, 24 h, and 48 h. PI-stained images after incubation of cells for 72 h in the presence of test compounds represent dead cells.

dependent anti-migratory activities of compounds **12** and **24** were observed as compared to the untreated cells under identical conditions up to a duration of 72 h. These results indicate that selenocyanates have the capability to suppress the movement and re-population of cells in the scratched wound region even up to 72 h. Similar dose-dependent anti-migratory activities of compounds **9–11** were also reported towards MDA-MB-231 cells for a duration of 24 h and 48 h.[17]

Study of cellular morphology upon selenocyanate treatment

The occurrence of apoptosis is accompanied by notable changes in the cellular morphology of cancerous cells. There are several techniques to understand/detect these changes confirming the mode of cell death. Cell shrinkage by a reduction of the volume of the cellular nucleus and cytoplasm is commonly associated with apoptotic cell death. The morphological changes upon cell death can be easily visualized under a microscope. In the present study, MDA-MB-231 cells were incubated with active selenocyanates **12** and **24** (10.0 μM) and the cellular morphology was visualized under a microscope after 24 h and 48 h. As shown in Fig. 8, significant visual changes were observed after 24 h and 48 h in the presence of compounds **12** and **24**. Visual changes in morphology during cell death are due to the formation of dead cell debris, which loses its adherent properties and becomes detached from the surface and floats randomly in the culture media. Significant cell death was found for the test compounds and it was enhanced with the incubation time as compared to the control experiments. In addition to visualization using a microscope, the incubated cells after 72 h were further stained with the nuclear staining fluorescent dye PI to detect the dead cell nuclei under an inverted fluorescence microscope. As PI cannot permeate through the cell membrane of live cells, it can selectively stain the nuclei of dead cells, indicating the extent of cell death. A significant number of dead cells were visualized upon PI-staining as shown in Fig. 8, supporting the occurrence of cell death.

Antioxidant activities of organoselenocyanates

A number of organoselenium compounds have been reported to show good to excellent antioxidant properties towards biological reactive oxygen species (ROS) such as hydrogen peroxide (H_2O_2), peroxynitrite ($ONOO^-$), hydroxyl radical ($OH^\bullet$) *etc*.[24] Although the *in vitro* antioxidant activity of organoselenocyanates has not been reported, we have taken the initiative to study their *in vitro* antioxidant properties.

Hydrogen peroxide scavenging activity. To understand the capability of test compounds to catalytically reduce H_2O_2, an *in vitro* assay was carried out spectrophotometrically using a glutathione (GSH)–glutathione disulfide (GSSG) coupled assay.[24b,25] To evaluate their relative antioxidant potentials, the rates were compared to that of the standard antioxidant organoselenium compound ebselen (2-phenyl-1,2-benzoselenazol-3-one, PZ-51). The activities of most of the selenocyanates were found to be much lower than that of ebselen under identical experimental conditions (Fig. S25, ESI†). This indicates that selenocyanates in the present study are relatively weaker antioxidants for the reduction of oxidants such as H_2O_2 in the presence of GSH as a co-substrate. Furthermore, we have carried out the reaction of standard selenocyanate **1** with aromatic thiol such as thiophenol (PhSH) and the product formation was monitored using ^{77}Se NMR spectroscopy to understand its reactivity towards thiols, which is an important step towards the antioxidant activity of organoselenium com-

pounds. Interestingly, the formation of the corresponding selenenyl sulfide ($PhCH_2Se$-SPh) upon the elimination of the cyano group from selenocyanate **1** was observed. This was confirmed by the appearance of a peak at 507 ppm with the disappearance of a peak due to compound **1** at 306 ppm in ^{77}Se NMR spectroscopic experiments (S41–S43, ESI†). A similar reaction of selenocyanate **1** with H_2O_2 led to the formation of oxidized species such as selenenic or seleninic acid derivatives. In this reaction, a highly de-shielded peak at 1330 ppm was observed, which could be ascribed to benzyl seleninic acid ($PhCH_2SeO_2H$).

Peroxynitrite scavenging assay. Peroxynitrite (PN) is a reactive nitrogen species (RNS), which is produced in the body and can lead to oxidation and nitration of bio-molecules, amino acid residues of proteins and enzymes.[26] A number of small molecules especially organochalcogen compounds have been developed as catalytic or stoichiometric scavengers of PN as monitored by the oxidation of dihydrorhodamine-123 (DHR-123) into the highly fluorescent rhodamine-123.[27] The scavenging potentials of selenocyanates were compared to that of ebselen, which has been shown to be a catalytic scavenger of PN.[27c] While ebselen exhibited strong scavenging activity (IC_{50} value: 4.2 μM), the activities of selenocyanates were significantly lower (Fig. S25, ESI†). Although a few selenocyanates such as **18**, **20** and **24** exhibited good scavenging activity under identical conditions, the IC_{50} values could not be calculated for some of the selenocyanates such as **1**, **3**, **16**, and **26**. These compounds exhibited some scavenging properties in the beginning; however, the inhibition remained less than 50% even up to 150–200 μM concentrations. A similar trend was observed for all the thiocyanates used in the present study. In general, the chalcogenocyanates used in the present study were found to be weaker scavengers of PN as compared to other organochalcogen compounds studied previously.[27]

Binding interaction with bovine serum albumin

As serum albumin is one of the highly abundant proteins in blood plasma of living systems and plays crucial roles in the transportation of several essential small molecules, drugs *etc.* by sequestering the latter at one site and specific release of the same at some other site, understanding the interaction of serum albumin with selenocyanates in this context is important to gain an insight into the pharmacodynamics of these compounds.[28] Bovine serum albumin (BSA) is very commonly used as a homology protein for human serum albumin (HSA) owing to its ready and cost-effective availability. Fluorescence quenching of BSA upon its interaction with small molecules is a simple but powerful tool for understanding the affinity of protein–ligand binding interactions. The fluorescence of BSA mainly arises due to the presence of tyrosine (Tyr) and two tryptophan (Trp) units, namely Trp-134 and Trp-212, located on the surface of sub-domain IB and in the hydrophobic pocket of sub-domain IIA, respectively. Therefore, the quenching of fluorescence of BSA upon binding with the drug/ligand indicates that the binding site of the protein may be in these domains.

In the present study, the binding interaction of selenocyanates with BSA was studied following an earlier reported procedure.[28] The BSA solution exhibits strong fluorescence emission at 344 nm upon excitation at 280 nm. The fluorescence intensity gradually decreases with an increase in the concentration of the test compounds without any shift in the emission λ_{max}, indicating that the compound quenches the intrinsic fluorescence of BSA in a static manner. The fluorescence quenching was performed by a titration method and the binding parameters such as the quenching constant (K_q) and Stern–Volmer constant (K_{SV}) were determined using the Stern–Volmer equation as shown in Table 2. The binding constant (K_a) and the number of binding sites (n) have been determined by using a Scatchard plot as reflected in Table 3. These results show that all the selenocyanate compounds exhibited very good binding affinity towards BSA with high K_{SV} and K_q values. The values of n for all the compounds are nearly 1.0, indicating a single molecular bond with BSA. Particularly, the most

Table 2 The binding parameters such as K_{SV} (Stern–Volmer constant) and K_q (quenching constant) of different test compounds with BSA as obtained from the Stern–Volmer equation[a]

Compound	K_{SV} ($\times 10^4$ M^{-1})	K_q ($\times 10^{12}$ M^{-1} S^{-1})	R^2
1	1.94	1.94	0.9907
3	2.81	2.81	0.9824
12	8.74	8.74	0.9910
16	2.75	2.75	0.9946
18	1.53	1.53	0.9958
20	4.71	4.71	0.9991
22	3.54	3.54	0.9969
24	4.81	4.81	0.9905
26	5.05	5.05	0.9699

[a] The quenching experiment was performed using a fluorescence spectrophotometer with excitation and emission wavelengths of 280 nm and 344 nm, respectively. BSA (10.0 μM) in Tris-HCl buffered saline (100 mM, pH 7.2) was titrated with increasing concentrations of test compounds (0.0–50.0 μM).

Table 3 The binding parameters such as K_b (binding constant) and n (number of molecules per unit protein) of different test compounds with BSA as determined by using a Scatchard plot[a]

Compound	K_b ($\times 10^4$ M^{-1})	n	R^2
1	0.89	0.93	0.9913
3	1.10	0.92	0.9695
12	1.04	0.81	0.9924
16	0.41	0.82	0.9993
18	5.08	1.11	0.9992
20	3.27	0.97	0.9988
22	3.36	0.99	0.9910
24	4.84	1.00	0.9879
26	0.10	0.64	0.9956

[a] The quenching experiment was performed using a fluorescencespectrophotometer with excitation and emission wavelengths of 280 nm and 344 nm, respectively. BSA (10.0 μM) in Tris-HCl buffered saline (100 mM, pH 7.2) was titrated with increasing concentrations of test compounds (0.0–50.0 μM).

active selenocyanate **12** exhibits much higher binding affinities as reflected by its higher K_{SV} and K_q values as compared to other analogous compounds. The higher binding affinity of **12** to BSA as compared to other compounds studied in this study is probably due to the presence of the 4-NO_2 group in addition to the selenocyanate moiety, which can have non-bonding interactions with the proximal amino acid residues in the binding site of BSA. The results from our study are in agreement with recent observations on the binding affinities of some organoselenium compounds with BSA.

It should be noted that the interaction of naphthalimide-based selenocyanates with BSA was studied in different binary solvents and a significant decrease in the fluorescence emission intensity of BSA was observed in the presence of selenocyanates.[29] A similar static interaction of selenadiazole derivatives with BSA with a good binding affinity has recently been reported by Chen and co-workers.[30] They showed that the binding of selenadiazole derivatives with serum albumin facilitated the drug transport through plasma and significantly enhanced their anti-tumor activities and cellular uptakes. Therefore, the efficient binding of compound **12** with BSA in our present study could be a good indicator of its enhanced anti-proliferative activity in breast cancer cells.

Analysis of some cellular proteins in MDA-MB-231 cells using western blot analysis

To understand the mode or pathway of anti-proliferative activities of active selenocyanates such as compound **12**, western blot analyses were performed on MDA-MB-231 cells. Some important cellular protein expression levels were estimated in the presence of active selenocyanate **12** at different concentrations (0.0, 0.25, 0.5, 1.0, 2.0 and 2.5 μM) and incubated for 24 h. Glyceraldehyde 3-phosphate dehydrogenase (GAPDH) was used as a housekeeping gene loading control for this experiment. As shown in Fig. 9, the expression levels of important proteins involved in cell survival, proliferation and angiogenesis such as COX-2, Survivin, Bcl-2 and VEGF-A, Akt, *p*-Akt *etc.* were studied in the presence of compound **12**. It is well-known that while COX-2 expression is crucial for invasive breast cancer and resistance to apoptosis, Survivin and Bcl-2 act as anti-apoptotic protein markers, responsible for the progression of carcinogenesis.[31] It is reflected in Fig. 9 that compound **12** reduces the levels of COX-2, Bcl-2 and Survivin in a dose-dependent manner and significant down-regulation was observed at higher concentrations such as 2.0 and 2.5 μM. These results indicate that the active selenocyanate **12** probably hase high impact on the expression level of important cellular proteins responsible for cancer progression. In contrast to these observations, the levels of proteins such as Akt, *p*-Akt (S476) and VEGF-A were almost unaltered in the presence of compound **12** up to a concentration of 2.5 μM.[32] These observations indicate that compound **12** exhibits anti-proliferative activity *via* the Akt-independent pathway. Although our results from western blot analysis on the levels of some key signaling molecules cannot be considered as conclusive remarks on the mode of action of compound **12**, these observations could be a platform for further studies on the molecular mechanisms of selenocyanates towards TNBC cells such as MDA-MB-231. More detailed mechanistic studies will be carried out with active compounds in a separate study in the future.

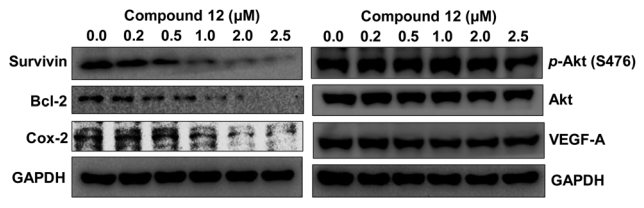

Fig. 9 Western blot analysis for the estimation of key protein expression levels in MDA-MB-231 cells in the presence of compound **12** at different concentrations (0.0, 0.2, 0.5, 1.0, 2.0 and 2.5 μM) for 24 h. Equal protein loading was confirmed by analysis of GAPDH expression.

Molecular interaction of selenocyanates with proteins

As compound **12** exhibited significant potency for the down-regulation of some key cancer-cellular proteins such as Survivin, Bcl-2 and COX-2, we carried out docking studies to understand the possible molecular interaction of **12** with these proteins. Additionally, the molecular interaction was also studied with BSA as these compounds exhibited good BSA-binding interactions. Compound **1** was used as a representative selenocyanate to obtain comparative interaction profiles. As shown in Table 4, compound **12** has much higher binding affinity than **1** towards BSA. This is represented by a higher binding energy and lower inhibitory constant of **12** as compared to **1**. Similar to BSA, the binding affinity of **12** was found to be significantly higher than that of **1** towards all the cellular proteins such as Survivin, Bcl-2 and COX-2, which are used in the present study.

The value of the inhibitory constant of compound **1** towards all four proteins was enormously decreased by the introduction of a simple nitro group at the 4-position of the phenyl ring of compound **1**. This increased affinity is probably

Table 4 The binding parameters such as binding energy (E_B), inhibitory constant (K_i) and the proximal amino acid residues of proteins involved in non-bonding interactions with ligands

Compound	Protein[a]	E_B (kcal mol^{-1})	K_i (μM)	Interactions
1	BSA	−4.2	829.4	—
	Survivin	−3.8	1750.0	L6.B, W10.A
	Bcl-2	−3.9	1310.0	Y67.B
	COX-2	−4.7	331.8	R376.B
12	BSA	−7.1	5.9	K114.A
	Survivin	−5.2	154.6	W10.A, L6.B
	Bcl-2	−6.0	39.5	K22.A, R26.A, R68.A
	COX-2	−6.3	24.6	R376.B, V538.B

[a] The docking study was performed with four proteins such as BSA (PDB: *4F5S*), Survivin (PDB: *1F3H*), Bcl-2 (PDB: *2 W3L*) and COX-2 (PDB: *5KIR*). The crystal structures of these proteins were collected from the RCSB database.

due to additional non-bonding interactions with the proximal amino acid residues of proteins involving the nitro group in compound **12**. Some representative interaction profiles are shown in the ESI† (Fig. S37–S40). These results support our experimental results that serum albumin may help in transporting these selenocyanates in the bloodstream and significant binding affinities reflect an effective interaction of compound **12** with cellular proteins.

Conclusions

In summary, we describe herein the synthesis of benzylic and mesitylenic organochalcogenocyanate compounds that have one or more selenocyanate or thiocyanate units. To the best of our knowledge, this is the first report to describe the synthesis of compounds having more than two chalcogenocyanate units in a single molecule. The compounds were evaluated for their anti-proliferative activities in three different breast cancer cells including TNBC cells (MDA-MB-231), for which treatment strategies are limited. This study reveals that selenocyanates exhibit much higher anti-proliferative activities than thiocyanates and the standard anti-cancer drug 5-FU. Furthermore, the activity of a simple benzyl selenocyanate could be significantly enhanced either by 4-nitro substitution at the phenyl ring or by derivatizing to mesitylenic selenocyanate. The 4-nitro substituted selenocyanate was very much selective towards TNBC cells over ER+ breast cancer cells and normal cells. Detailed studies reveal that the apoptotic nature of selenocyanates is associated with modulation of cellular morphology and cell cycle arrest at S-phase. Furthermore, our study also demonstrated the possible anti-invasive activity of these selenocyanates through the inhibition of cellular migration. However, the active selenocyanates were found to have weak antioxidant activities. Additionally, an effective binding interaction of active selenocyanate with serum albumin indicates its feasible transport in the bloodstream for its enhanced anti-cancer properties. Further mechanistic studies with the most active compound demonstrate that selenocyanates exhibit anti-proliferative activities by down-regulating key cellular proteins such as Survivin, Bcl-2 and COX-2, which was further supported by effective protein–ligand interactions as predicted by molecular docking studies. Although the exact mechanism of action of these selenocyanates could not be highlighted here, results from this study would be helpful in designing a suitable selenocyanate as an anti-proliferative and chemopreventive drug candidate in the future.

Experimental section

Materials and methods

All commercial reagents were used as delivered, without further purification. Solvents used for purification (ethyl acetate, *n*-hexane, and petroleum ether 60–80) were freshly distilled before use. Dry solvents were used as applicable for the air and moisture sensitive reactions. All melting points were measured with a Büchi Melting Point B540 apparatus and the values were uncorrected. Thin layer chromatographic (TLC) analyses were carried out on pre-coated silica gel on aluminium sheets. The NMR spectra were measured with a Bruker Ascend™ 600 spectrometer (^{1}H NMR at 600 MHz, ^{13}C NMR at 150 MHz and ^{77}Se NMR at 114 MHz) or a Varian Mercury Plus 400 MHz NMR spectrometer. Chemical shifts are cited with respect to Me_4Si (^{1}H and ^{13}C) as an internal standard and Me_2Se (^{77}Se) as an external standard. High resolution mass spectra (HR-MS) and liquid chromatography mass spectra (LC-MS) were obtained using an Agilent 6520 Accurate-Mass Quadrupole Time-of-Flight (Q-TOF) LC/MS spectrometer. IR spectra were recorded with a PerkinElmer Spectrum Two FT-IR spectrometer.

General procedure 1[20]

To a stirred solution of benzylic or mesitylenic halides in dry acetonitrile was added a solution of potassium selenocyanate (KSeCN) in acetonitrile and the mixture was stirred at room temperature. The appearance of a white precipitate (inorganic salt) soon after the addition of KSeCN indicated the progress of the reaction with the formation of selenocyanates. The progress and completion of the reaction was monitored by the thin layer chromatographic (TLC) method.

General procedure 2[21]

To a stirred solution of benzylic or mesitylenic halides in dry methanol was added a solution of potassium thiocyanate (KSCN) in methanol and the mixture was stirred under reflux. The appearance of a white precipitate (inorganic salt) soon after the addition of KSCN indicated the progress of the reaction with the formation of thiocyanates. The progress and completion of the reaction was monitored by the thin layer chromatographic (TLC) method.

Work-up method 1. The reaction mixture was poured into cold distilled water and stirred for 30 minutes. The precipitate was filtered off and washed with water to remove any inorganic salt. The crude solid was dried and purified by the column chromatographic method.

Work-up method 2. The solvent was evaporated under reduced pressure and the residue was dissolved in ethyl acetate and diluted with water. The aqueous layer was extracted with ethyl acetate (3 times). The combined organic layer was washed with brine and dried over sodium sulfate and filtered off. The solvent was evaporated under reduced pressure to afford the crude product. The crude product was purified by the column chromatographic method.

Synthesis of compound 1

Prepared following the general method 1 using benzyl bromide (0.40 mL, 3.47 mmol) and KSeCN (0.50 g, 3.16 mmol) in acetonitrile (15 mL). The reaction mixture was stirred at room temperature for 1 h. Work-up method 1 was used to afford the crude product as an off-white solid. The crude solid was dried and purified by silica gel column chromatography using ethyl acetate and petroleum ether 60–80 as eluents.

R_f = 0.5 (4% ethyl acetate in petroleum ether 60–80). Yield: 0.39 g (59%). M.P.: 73–75 °C. ^{1}H NMR ($CDCl_3$, 600 MHz): δ (ppm) = 7.39–7.33 (m, 5H), 4.31 (s, 2H); ^{13}C NMR ($CDCl_3$, 150 MHz): δ (ppm) = 135.7, 129.4, 129.2, 128.9, 102.2, 33.0; ^{77}Se NMR ($CDCl_3$, 114 MHz): δ (ppm) = 283. IR (KBr pellet, cm^{-1}): 2146 (s), 1491 (m), 1454 (m), 1217 (m), 1191 (m), 1069 (m). ESI-MS m/z calcd for C_8H_7NSe $[M + Na]^+$: 219.9641; obs: 220.0526.

Synthesis of compound 2

Prepared following the general method 2 using benzyl bromide (0.40 g, 2.34 mmol) and KSCN (0.34 g, 3.51 mmol) in methanol (5 mL) and the mixture was refluxed for 3 h. Work-up method 2 was used to afford the crude product as yellow solid. The crude solid was dried and purified using silica gel column chromatography using ethyl acetate and petroleum ether 60–80 as eluents. R_f = 0.7 (10% ethyl acetate in petroleum ether). Yield: 0.2 g (57%). M.P.: 39–41 °C. ^{1}H NMR ($CDCl_3$, 600 MHz): δ (ppm) = 7.41–7.35 (m, 5H), 4.17 (s, 2H); ^{13}C NMR ($CDCl_3$, 150 MHz): δ (ppm) = 134.3, 129.1, 129.0, 128.9, 112.0, 38.3; IR (KBr pellet, cm^{-1}): 2991 (m), 2147 (s), 1493 (m). ESI-MS (LC-MS) m/z calcd for C_8H_7NS $[M + Na]^+$: 172.02; obs: 172.00.

Synthesis of compound 3

Prepared following the general method 1 using 1,4-phenylene-bis(methylene) bromide (0.40 g, 1.52 mmol) and KSeCN (0.5 g, 3.47 mmol) in acetonitrile (20 mL). The reaction was stirred at room temperature for 2 h. Work-up method 2 was used to afford the crude product as a white amorphous solid. The crude solid was dried and purified by silica gel column chromatography using ethyl acetate and petroleum ether. R_f = 0.5 (36% ethyl acetate in petroleum ether); yield: 0.46 g (95%). M.P. = 152–155 °C. ^{1}H NMR ($CDCl_3$, 600 MHz): δ (ppm) = 7.38 (s, 4H), 4.28 (s, 4H); ^{13}C NMR ($CDCl_3$, 150 MHz): δ (ppm) = 136.4, 130.0, 101.8, 32.3; ^{77}Se NMR ($CDCl_3$, 114 MHz): δ (ppm) = 293. IR (KBr pellet, cm^{-1}): 2924 (s), 2853 (m), 2147 (s), 1426 (m), 1190 (m), 1092 (s). ESI-MS m/z calcd for $C_{10}H_8N_2Se_2$ $[M + H]^+$: 316.9096; obs: 316.9086.

Synthesis of compound 4

Prepared following the general method 2 using 1,4-phenylene-bis(methylene) bromide (0.40 g, 1.52 mmol), and KSCN (0.37 g, 3.79 mmol) in methanol (5 mL). The reaction was refluxed at 65 °C for 4 h. Work-up method 2 was used to afford the crude product as a white solid. The crude solid was dried and purified by silica gel column chromatography using ethyl acetate and petroleum ether. R_f = 0.3 (10% ethyl acetate in petroleum ether). Yield: 0.26 g (79%). M.P. = 134–136 °C. ^{1}H NMR ($CDCl_3$, 600 MHz): δ (ppm) = 7.40 (s, 4H), 4.15 (s, 4H); ^{13}C NMR ($CDCl_3$, 150 MHz): δ (ppm) = 135.3, 129.8, 111.7, 37.7; IR (KBr pellet, cm^{-1}): 2924 (w), 2154 (s), 1426 (m), 1245 (m); ESI-MS m/z calcd for $C_{10}H_8N_2S_2$ $[M + Na]^+$: 243.0027; obs: 243.0188.

Synthesis of compound 12

Prepared following the general method 1 using 4-nitrobenzyl bromide (0.42 g, 1.85 mmol) and KSeCN (0.40 g, 2.78 mmol) in acetonitrile (20 mL). The reaction mixture was stirred at room temperature for 4 h. Work-up method 1 was used to afford the crude product as an off-white crystalline solid. The crude solid was dried and purified by silica gel column chromatography using ethyl acetate and petroleum ether 60–80 as eluents. R_f = 0.7 (25% ethyl acetate in petroleum ether 60–80). Yield: 0.39 g (83%). M.P. = 120–123 °C. ^{1}H NMR ($CDCl_3$, 600 MHz): δ (ppm) = 8.25–8.24 (d, J = 6.0 Hz, 2H), 7.55–7.54 (d, J = 6.0 Hz, 2H), 4.30 (s, 2H); ^{13}C NMR ($CDCl_3$, 150 MHz): δ (ppm) = 148.1, 143.3, 130.1, 124.6, 100.8, 31.1; ^{77}Se NMR ($CDCl_3$, 114 MHz): δ (ppm) = 312; IR (KBr pellet, cm^{-1}): 2924 (s), 2146 (m), 1597 (m), 1519 (s), 1342 (s). ESI-MS m/z calcd for $C_8H_6N_2O_2Se$ $[M + H]^+$: 242.9673; obs: 242.2854.

Synthesis of compound 13

Prepared following the general method 2 using 4-nitrobenzyl bromide (0.45 g, 2.08 mmol) and KSCN (0.30 g, 3.12 mmol) in methanol (5 mL). The reaction mixture was refluxed at 65 °C for 4 h. Work-up method 2 was used to afford the crude product as an off-white crystalline solid. The crude solid was dried and purified by neutral alumina column chromatography using ethyl acetate and petroleum ether 60–80 as eluents. R_f = 0.3 (10% ethyl acetate in petroleum ether 60–80). Yield: 0.17 g (43%). M.P. = 82–84 °C. ^{1}H NMR ($CDCl_3$, 600 MHz): δ (ppm) = 8.28–8.27 (d, J = 6.0 Hz, 2H), 7.57–7.56 (d, J = 6.0 Hz, 2H), 4.20 (s, 2H); ^{13}C NMR ($CDCl_3$, 150 MHz): δ (ppm) = 148.1, 141.6, 130.0, 124.4, 110.8, 37.0; IR (KBr pellet, cm^{-1}): 3106 (w), 2152 (m), 1515 (s), 1344 (s); ESI-MS m/z calcd for $C_8H_6N_2O_2S$ $[M + NH_4]^+$: 212.0494; obs: 212.0220.

Synthesis of compound 14

Prepared following the general method 1 using 1,2-phenylene-bis(methylene) bromide (0.40 g, 1.52 mmol), and KSeCN (0.50 g, 3.47 mmol) in acetonitrile (15 mL). The reaction was stirred at room temperature for 2 h. Work-up method 1 was used to afford the crude product as a white crystalline solid. The crude solid was dried and purified by neutral alumina column using ethyl acetate and hexane. R_f = 0.5 (50% ethyl acetate in hexane). Yield: 0.41 g (88%). M.P. = 105–107 °C. ^{1}H NMR (DMSO-d_6, 600 MHz): δ (ppm) = 7.34–7.31 (m, 4H), 4.43 (s, 4H); ^{13}C NMR (DMSO-d_6, 150 MHz): δ (ppm) = 136.9, 131.8, 129.1, 105.2, 30.3; ^{77}Se NMR (DMSO-d_6, 114 MHz): δ (ppm) = 314; IR (KBr pellet, cm^{-1}): 2923 (m), 2148 (s), 1451 (m), 1194 (m). ESI-MS m/z calcd for $C_{10}H_8N_2Se_2$ $[M + Na]^+$: 337.8916; obs: 337.4143.

Synthesis of compound 15

Prepared following the general method 2 using 1,2-phenylene-bis(methylene) bromide (0.40 g, 1.52 mmol), and KSCN (0.37 g, 3.79 mmol) in methanol (5 mL). The reaction was refluxed at 65 °C for 5 h. Work-up method 2 was used to afford the crude product as a white solid. The crude solid was dried

and purified by neutral alumina column using ethyl acetate and petroleum ether. R_f = 0.6 (20% ethyl acetate in petroleum ether). Yield: 0.26 g (78%). M.P. = 77–79 °C. ^{1}H NMR ($CDCl_3$, 600 MHz): δ (ppm) = 7.45–7.41 (m, 4H), 4.31 (s, 4H); ^{13}C NMR ($CDCl_3$, 150 MHz): δ (ppm) = 132.7, 131.7, 130.2, 111.0, 35.1; IR (KBr pellet, cm^{-1}): 3003 (m), 2152 (s), 1427 (m), 1237 (s); ESI-MS *m*/*z* calcd for $C_{10}H_8N_2S_2$ $[M + NH_4]^+$: 238.0473; obs: 238.0462.

Synthesis of compound 16

Prepared following the general method 1 using 1,4-bis(bromomethyl)-2,5-dimethylbenzene (0.30 g, 1.03 mmol), and KSeCN (0.32 g, 2.26 mmol) in acetonitrile (10 mL). The reaction was stirred at room temperature for 2 h. Work-up method 1 was used to afford the crude product as a yellow amorphous solid. The crude solid was dried and purified by silica gel column chromatography using ethyl acetate and petroleum ether. R_f = 0.5 (25% ethyl acetate in hexane). Yield: 0.23 g (65%). M.P. = 207–209 °C. ^{1}H NMR (DMSO-d_6, 600 MHz): δ (ppm) = 7.13 (s, 2H), 4.32 (s, 4H), 2.29 (s, 6H); ^{13}C NMR (DMSO-d_6, 150 MHz): δ (ppm) = 136.1, 134.6, 133.0, 105.2, 31.1, 19.1; ^{77}Se NMR (DMSO-d_6, 114 MHz): δ (ppm) = 292; IR (KBr pellet, cm^{-1}): 2953 (m), 2922 (s), 2854 (m), 2147 (s), 1447 (m). ESI-MS *m*/*z* calcd for $C_{12}H_{12}N_2Se_2$ $[M + NH_4]^+$: 361.9675; obs: 361.9665.

Synthesis of compound 17

Prepared following the general method 2 using 1,4-bis(bromomethyl)-2,5-dimethylbenzene (0.40 g, 1.37 mmol), and KSCN (0.33 g, 3.42 mmol) in methanol (5 mL). The reaction was refluxed at 65 °C for 5 h. Work-up method 2 was used to afford the crude product as a white solid. The crude solid was dried and purified by silica gel column chromatography using ethyl acetate and petroleum ether. R_f = 0.5 (20% ethyl acetate in petroleum ether). Yield: 0.17 g (49%). M.P. = 194–196 °C. ^{1}H NMR ($CDCl_3$, 400 MHz): δ (ppm) = 7.14 (s, 2H), 4.16 (s, 4H), 2.38 (s, 6H); ^{13}C NMR (DMSO-d_6, 150 MHz): δ (ppm) = 134.3, 133.9, 132.4, 112.6, 34.8, 18.1, IR (KBr pellet, cm^{-1}): 2923 (m), 2151 (s), 1432 (w); ESI-MS *m*/*z* calcd for $C_{12}H_{12}N_2S_2$ $[M + NH_4]^+$: 266.0786; obs: 266.0838.

Synthesis of compound 18

Prepared following the general method 1 using 1,3-phenylenebis(methylene) bromide (0.40 g, 1.52 mmol), and KSeCN (0.50 g, 3.47 mmol) in acetonitrile (20 mL). The reaction was stirred at room temperature for 2 h. Work-up method 2 was used to afford the crude product as a pale yellow solid. The crude solid was dried and purified by silica gel column chromatography using ethyl acetate and petroleum ether. R_f = 0.4 (32% ethyl acetate in petroleum ether). Yield: 0.46 g (97%). M.P. = 108–110 °C. ^{1}H NMR ($CDCl_3$, 600 MHz): δ (ppm) = 7.39–7.33 (m, 4H), 4.27 (s, 4H); ^{13}C NMR ($CDCl_3$, 150 MHz): δ (ppm) = 136.9, 130.2, 129.6, 129.5, 101.9, 32.3; ^{77}Se NMR ($CDCl_3$, 114 MHz): δ (ppm) = 295; IR (KBr pellet, cm^{-1}): 2923 (m), 2150 (s), 1200 (m). ESI-MS *m*/*z* calcd for $C_{10}H_8N_2Se_2$ $[M + Na]^+$: 337.0937; obs: 337.1142.

Synthesis of compound 19

Prepared following the general method 2 using 1,3-phenylenebis(methylene) bromide (0.40 g, 1.52 mmol), and KSCN (0.44 g, 4.55 mmol) in methanol (5 mL). The reaction was refluxed at 65 °C for 5 h. Work-up method 2 was used to afford the crude product as a yellow solid. The crude solid was dried and purified by neutral alumina column using ethyl acetate and petroleum ether. R_f = 0.6 (30% ethyl acetate in petroleum ether). Yield: 0.26 g (78%). M.P. = 60–62 °C. ^{1}H NMR ($CDCl_3$, 600 MHz): δ (ppm) = 7.45–7.37 (m, 4H), 4.16 (s, 4H); ^{13}C NMR ($CDCl_3$, 150 MHz): δ (ppm) = 135.5, 130.0, 129.5, 129.4, 111.6, 37.8; IR (KBr pellet, cm^{-1}): 2992 (m), 2151 (s), 1429 (m), 1240 (m); ESI-MS *m*/*z* calcd for $C_{10}H_8N_2S_2$ $[M + NH_4]^+$: 238.0473; obs: 238.0469.

Synthesis of compound 20

Prepared following the general method 1 using 1,3-bis(bromomethyl)mesitylene (0.50 g, 1.63 mmol), and KSeCN (0.50 g, 3.47 mmol) in acetonitrile (15 mL). The reaction was stirred at room temperature for 2 h. Work-up method 2 was used to afford the crude product as a white amorphous solid. The crude solid was dried and purified by silica gel column chromatography using ethyl acetate and petroleum ether. R_f = 0.5 (26% ethyl acetate in petroleum ether), yield: 0.52 g (89%). M.P. = 154–157 °C; ^{1}H NMR ($CDCl_3$, 600 MHz): δ (ppm) = 6.95 (s, 1H), 4.48 (s, 4H), 2.47 (s, 3H), 2.40 (s, 6H); ^{13}C NMR ($CHCl_3$, 150 MHz): δ (ppm) = 138.6, 137.2, 131.6, 129.9, 101.7, 29.0, 20.3, 16.1; ^{77}Se NMR (DMSO-d_6, 114 MHz): δ (ppm) = 252; IR (KBr pellet, cm^{-1}): 2916 (w), 2148 (s), 1458 (m), 1190 (s); ESI-MS *m*/*z* calcd for $C_{13}H_{14}N_2Se_2$ $[M + NH_4]^+$: 375.9831; obs: 375.9830.

Synthesis of compound 21

Prepared following the general method 2 using 1,3-bis(bromomethyl)mesitylene (0.40 g, 1.31 mmol), and KSCN (0.38 g, 3.92 mmol) in methanol (5 mL). The reaction was refluxed at 65 °C for 5 h. Work-up method 2 was used to afford the crude product as a white solid. The crude solid was dried and purified by silica gel column chromatography using ethyl acetate and petroleum ether. R_f = 0.8 (30% ethyl acetate in petroleum ether). Yield: 0.11 g (32%). M.P. = 107–109 °C. ^{1}H NMR ($CDCl_3$, 600 MHz): δ (ppm) = 6.98 (s, 1H), 4.37 (s, 4H), 2.48 (s, 3H), 2.41 (s, 6H); ^{13}C NMR ($CDCl_3$, 150 MHz): δ (ppm) = 138.8, 137.4, 131.4, 129.0, 111.8, 33.6, 20.0, 15.8; IR (KBr pellet, cm^{-1}): 2926 (w), 2147 (s), 1380 (w); ESI-MS *m*/*z* calcd for $C_{13}H_{14}N_2S_2$ $[M + Na]^+$: 285.0496; obs: 285.0485.

Synthesis of compound 22

Prepared following the general method 1 using 1,3,5-tris (bromomethyl) benzene (0.2 g, 0.56 mmol), and KSeCN (0.26 g, 1.8 mmol) in acetonitrile (7 mL). The reaction was stirred at room temperature for 2 h. Work-up method 2 was used to afford the crude product as an off-white crystalline solid. The crude solid was dried and purified by silica gel column chromatography using ethyl acetate and hexane. R_f = 0.6 (50% ethyl

acetate in hexane). Yield: 0.13 g (53%). M.P. = 158–160 °C. ^{1}H NMR (DMSO-d_6, 600 MHz): δ (ppm) = 7.30 (s, 3H), 4.29 (s, 6H); ^{13}C NMR (DMSO-d_6, 150 MHz): δ (ppm) = 139.7, 129.4, 105.5, 32.9; ^{77}Se NMR (DMSO-d_6, 114 MHz): δ (ppm) = 315; IR (KBr pellet, cm^{-1}): 2925 (m), 2151 (s), 1455 (m), 1430 (m), 1196 (m). ESI-MS *m*/*z* calcd for $C_{12}H_9N_3Se_3$ $[M + Na]^+$: 455.0897; obs: 455.2540.

Synthesis of compound 23

Prepared following the general method 2 using 1,3,5-tris (bromomethyl)benzene (0.20 g, 0.70 mmol), and KSCN (0.22 g, 2.8 mmol) in methanol (3 mL). The reaction was refluxed at 65 °C for 5 h. Work-up method 2 was used to afford the crude product as a white solid. The crude solid was dried and purified by silica gel column chromatography using ethyl acetate and petroleum ether. R_f = 0.4 (30% ethyl acetate in petroleum ether). Yield: 71 mg (44%). M.P. = 112–114 °C. ^{1}H NMR ($CDCl_3$, 400 MHz): δ (ppm) = 7.39 (s, 3H), 4.17 (s, 6H); ^{13}C NMR ($CDCl_3$, 150 MHz): δ (ppm) = 136.8, 129.9, 111.3, 37.4; IR (KBr pellet, cm^{-1}): 2989 (w), 2156 (s), 1431 (m); ESI-MS *m*/*z* calcd for $C_{12}H_9N_3S_3$ $[M + NH_4]^+$: 309.0302; obs: 309.3262.

Synthesis of compound 24

Prepared following the general method 1 using 1,3,5-tris (bromomethyl)mesitylene (0.40 g, 1.00 mmol), and KSeCN (0.58 g, 4.03 mmol) in acetonitrile (15 mL). The reaction was stirred at room temperature for 2 h. Work-up method 2 was used to afford the crude product as a white amorphous solid. The crude solid was dried and purified by silica gel column chromatography using ethyl acetate and petroleum ether. R_f = 0.5 (40% ethyl acetate in petroleum ether). Yield: 0.42 g (88%). M.P. = 160–163 °C. ^{1}H NMR (DMSO-d_6, 600 MHz): δ (ppm) = 4.52 (s, 6H), 2.41 (s, 9H); ^{13}C NMR (DMSO-d_6, 150 MHz): δ (ppm) = 138.0, 132.6, 104.3, 29.9, 17.4; ^{77}Se NMR (DMSO-d_6, 114 MHz): δ (ppm) = 251; IR (KBr pellet, cm^{-1}): 2923 (s), 2853 (m), 2148 (m), 1730 (m), 1461 (m), 1191 (m); ESI-MS *m*/*z* calcd for $C_{15}H_{15}N_3Se_3$ $[M + Na]^+$: 497.1695; obs: 497.8654.

Synthesis of compound 25

Prepared following the general method 2 using 1,3,5-tris (bromomethyl)mesitylene (0.50 g, 1.25 mmol), and KSCN (0.49 g, 5.01 mmol) in methanol (6 mL). The reaction was refluxed at 65 °C for 4 h. Work-up method 2 was used to afford the crude product as a white solid. The crude solid was dried and purified by silica gel column chromatography using ethyl acetate and petroleum ether. R_f = 0.4 (20% ethyl acetate in petroleum ether). Yield: 0.36 g (86%). M.P. = 146–148 °C. ^{1}H NMR ($CDCl_3$, 400 MHz): δ (ppm) = 4.40 (s, 6H), 2.53 (s, 9H); ^{13}C NMR ($CDCl_3$, 150 MHz): δ (ppm) = 138.7, 130.2, 111.3, 50.9, 33.9, 16.7; IR (KBr pellet, cm^{-1}): 2957 (w), 2154 (s), 2141 (s), 1443 (m), 1232 (s); ESI-MS *m*/*z* calcd for $C_{15}H_{15}N_3S_3$ $[M + Na]^+$: 356.0326; obs: 356.0300.

Synthesis of compound 26

Prepared following the general method 1 using 1,2,3,4,5,6-hexakis(bromomethyl)benzene (0.10 g, 0.16 mmol), and KSeCN (0.15 g, 0.97 mmol) in acetonitrile (10 mL). The reaction was stirred at room temperature for 7 h. Work-up method 1 was used to afford the crude product as a white solid, which was insoluble in water and non-polar organic solvents such as dichloromethane, ethyl acetate, methanol and acetonitrile. The product could not be eluted on a silica gel TLC plate. Yield: 0.47 g (93%). M.P. = 224–227 °C. ^{1}H NMR (DMSO-d_6, 600 MHz): δ (ppm) = 4.69 (s, 12H); ^{13}C NMR (DMSO-d_6, 150 MHz): δ (ppm) = 137.6, 104.4, 27.9; ^{77}Se NMR (DMSO-d_6, 114 MHz): δ (ppm) = 305; IR (KBr pellet, cm^{-1}): 2924 (m), 2162 (s), 2148 (s), 1493 (m), 1169 (s); ESI-MS *m*/*z* calcd for $C_{18}H_{12}N_6Se_6$ $[M + H]^+$: 792.6193; obs: 793.3620.

Synthesis of compound 27

To a stirred solution of 1,2,3,4,5,6-hexakis(bromomethyl) benzene (0.15 g, 0.24 mmol) in dry MeOH was added a solution of KSCN (0.15 g, 1.5 mmol) in dry MeOH (6 mL) and the solution was refluxed for 7 h at 65 °C. The progress of the reaction was monitored by the thin layer chromatographic (TLC) method. After completion, the solvent was evaporated under reduced pressure. The residue was stirred with water to dissolve the inorganic salts, followed by filtration and subsequent drying under reduced pressure to yield the crude product. R_f = 0.6 (65% ethyl acetate in petroleum ether). Yield: 70 mg (59%). M.P. = 190–192 °C. ^{1}H NMR (DMSO-d_6, 600 MHz): δ (ppm) = 4.81 (s, 12H); ^{13}C NMR (DMSO-d_6, 150 MHz): δ (ppm) = 137.1, 112.4, 31.7; IR (KBr pellet, cm^{-1}): 2924 (w), 2161 (s), 2147 (s), 1190 (m); ESI-MS *m*/*z* calcd for $C_{18}H_{12}N_6S_6$ $[M + NH_4]^+$: 521.9791; obs: 521.9907.

Cell culture

The TNBC cell line MDA-MB-231 was a kind gift from Dr Anil Mukund Limaye, Associate Professor, Department of Biosciences and Bioengineering, Indian Institute of Technology Guwahati (IIT Guwahati), Assam, India. RPMI 1640 medium (Gibco) added with 10% fetal bovine serum (FBS) (Gibco) and 1% Pen-Strep (Gibco) was used as a nutrient supplement for the MDA-MB-231 cells. T-47D cells were procured from Dr VGM Naidu, Associate Professor, Department of Pharmacology & Toxicology, National Institute of Pharmaceutical Education and Research (NIPER) Guwahati. MCF-7 and L-132 cells were purchased from National Centre for Cell Science (NCCS), Pune, India. The T-47D, MCF-7 and L-132 cells were cultured in DMEM (Gibco) supplemented with 10% fetal bovine serum (FBS) (Gibco) and 1% Pen-Strep (Cell Clone). All the cells were maintained in a CO_2-regulated humidified (95% air/5% CO_2 atmosphere) incubator at 37 °C.

MTT assay

The cells were plated in 96-well culture plates at a density of 2×10^3 cells per 100 μl per well for L-132 cells and 4×10^3 cells per 100 μl per well for all other cells and treated with 0.0, 1.0, 5.0, 10.0 and 25.0 μM of test compounds for 0 h (Set 1) and 72 h (Set 2). At the end of the treatment period, 10.0 μL of 5.0 mg mL^{-1} of MTT was added to the plate (Set 1) and incubated for 2 h. Following the 2 h incubation, the culture

medium from the plate was removed and the purple formazan crystals were dissolved using 100 μl of DMSO (Merck Life Science Pvt Ltd) and the absorbance at 570 nm was measured using a microplate reader (TECAN Infinite 200 PRO multimode reader). In Set 2, a similar MTT treatment protocol was followed only after 72 h. The mean OD values of a 0 h plate (Set 1) were subtracted from the mean OD values of identical wells at a 72 h plate (Set 2) ΔOD and the inhibition of proliferation was calculated keeping the ΔOD of the untreated control as 100%.

Propidium iodide (PI) flow cytometric assay

5×10^4 cells per 2 mL per well were plated in 6-well plates and treated with 0.0, 10.0 and 25.0 μM of selected selenocyanates (**1**, **3**, **18**, **20** and **24**) and 0.0, 5.0 and 10.0 μM of compound **12** for 72 h. At the end of 72 h, the cells were harvested and washed with PBS (1X), stained with 5.0 μl of 1.0 mg mL^{-1} propidium iodide (PI) (Sigma-Aldrich), a nucleic acid intercalating fluorescent dye, and analysed using a BD FACSCalibur™ instrument (BD Biosciences).

Cell cycle analysis

1×10^5 cells per 2 mL per well were seeded in 6-well plates and treated with 0.0, 1.0 and 5.0 μM of compounds **12** and **24** and incubated for 24 h. Following the 24 h drug treatment, the cells were collected; washed with PBS (1X); fixed with ice-cold 70% ethanol at −20 °C for 30 min; again washed with PBS (1X) and stained with PI/RNase staining buffer (BD Biosciences) for 10 min at room temperature. The prepared samples were then analysed using a BD FACSCalibur™ instrument (BD Biosciences).

Wound healing (scratch) assay

MDA-MB-231 cells were seeded in a 24-well plate at a concentration of 1.5×10^5 cells per 2 mL per well and incubated in a CO_2 incubator at 37 °C to form a monolayer of cells. After the monolayer formation, the cells were pre-incubated in serum free medium for 6 h. Using a 100 μl tip, a scratch was made on the monolayer and the debris was removed by washing with PBS (1X). Then, the cells were re-incubated with serum free medium and treated with 0.0, 1.0 and 2.5 μM of active selenocyanates **12** and **24**. Images of the scratch were captured at regular time intervals (0, 24, 48 and 72 h) using a Nikon inverted microscope and a camera. The extent of wound healing denotes the anti-migratory effect of the compounds tested.

Assessment of cellular morphology and apoptotic bodies

5×10^4 cells per 1 mL per well were plated in 24-well plates and treated with 0.0 and 10.0 μM of compounds **12** and **24**. The cells were observed for any morphological changes and the change in morphology was captured at a regular time intervals (0, 24 and 48 h) using a Nikon inverted microscope and a camera. After 72 h, the formation of apoptotic nuclei was analysed by staining the cells with 5 μl of 1 mg mL^{-1} PI and images were taken using an Eclipse Ti-S inverted fluorescence microscope.

Western blot analysis

MDA-MB-231 cells were treated with 0.0, 0.2, 0.5, 1.0, 2.0 and 2.5 μM of compound **12** for 24 h and the whole cell protein lysate was made using lysis buffer (20 μM HEPES buffer, 1 M NaCl, 0.5 M EDTA, 1 mg mL^{-1} leupeptin, 100 mM PMSF, 5 mg mL^{-1} aprotinin, 1 M DTT and 0.1% (v/v) Triton-X100). Total protein concentration was estimated with the Bradford protein assay; 20 μg of protein lysate was loaded and separated on a 12% sodium dodecyl sulfate (SDS)–polyacrylamide gel by electrophoresis and transferred to a nitrocellulose membrane. Protein transfer was confirmed by Ponceau-S (HiMedia) staining. The blots were blocked with 5% non-fat dry milk or BSA in 1X TBST buffer for 2 h at room temperature and incubated with an appropriate dilution of the primary antibodies specific for COX-2, Survivin, Bcl-2, VEGF-A, Akt, p-Akt and GAPDH (Cell Signaling Technology) overnight at 4 °C. Following the primary antibody incubation, the blots were washed and incubated with HRP-conjugated secondary antibodies (Abcam) for 2 h and developed with an Optiblot ECL Detect Kit (Abcam) and ChemiDoc™ XRS System (Bio-Rad). The housekeeping gene GAPDH was used as a loading control.

Docking studies

AutoDock 4.2 MGL Tools and Lamarckian Generic Algorithm (LGA) were used for protein-fixed ligand-flexible docking calculations.[33] Auto grid version 4.2 was used to calculate the grid parameters and the grid size was set at 40 × 40 × 40 points with a grid spacing of 0.375 Å, 0.519 Å, 0.375 Å, and 0.5916 Å for Bcl-2, BSA, COX-2 and Survivin, respectively. Twenty search attempts (*i.e.*, ga_run parameter) were performed for each ligand. The maximum number of energy evaluations before the termination of the LGA run was 250 000 and the maximum number of generations of LGA run before termination was 27 000. Other docking parameters were set to the default values of AutoDock 4.2 program.

Conflicts of interest

There are no conflicts to declare.

Acknowledgements

This project was supported by the Science and Engineering Research Board (SERB), India. KPB acknowledges SERB for the award of a DST-INSPIRE Faculty Fellowship (Ref.: IFA12-CH-68) and IIT Guwahati for a Start-Up Research Grant. We thank the Central Instruments Facility (CIF), IIT Guwahati for NMR and the DST-FIST for ESI-MS facilities. KB, GP, DB and SS thank IIT Guwahati for their research fellowships.

References

1 E. M. Ward, C. E. DeSantis, C. C. Lin, J. L. Kramer, A. Jemal, B. Kohler, O. W. Brawley and T. Gansler, *CA-Cancer J. Clin.*, 2015, **65**, 481–495.

2 T. W. Lin, H. T. Chang, C. H. Chen, C. H. Chen, S. W. Lin, T. L. Hsu and C. H. Wong, *J. Am. Chem. Soc.*, 2015, **137**, 9685–9693.
3 K. Nohara, F. Wang and S. Spiegel, *Breast Cancer Res. Treat.*, 1998, **48**, 149–157.
4 J. P. Jogy and G. Giles, *Free Radicals Biol. Med.*, 2017, **112**, 98–99.
5 (*a*) K. A. Conklin, *J. Nutr.*, 2004, **134**, 3201s–3204s; (*b*) S. Arora, A. Bhardwaj, S. Singh, S. K. Srivastava, S. McClellan, C. S. Nirodi, G. A. Piazza, W. E. Grizzle, L. B. Owen and A. P. Singh, *J. Biol. Chem.*, 2013, **288**, 21197–21207; (*c*) S. Arora, A. Bhardwaj, S. Singh, S. K. Srivastava, S. McClellan, W. E. Grizzle, L. B. Owen and A. P. Singh, *Cancer Res.*, 2013, **73**, 4794.
6 S. Shaaban, M. A. Arafat and W. S. Hamama, *ARKIVOC*, 2014, 470–505.
7 (*a*) D. Medina and D. G. Morrison, *Pathol. Immunopathol. Res.*, 1988, **7**, 187–199; (*b*) D. Medina and H. W. Lane, *Biol. Trace Elem. Res.*, 1983, **5**, 297–306; (*c*) G. N. Schrauzer, D. A. White and C. J. Schneider, *Bioinorg. Chem.*, 1976, **6**, 265–270; (*d*) C. Ip, K. El-Bayoumy, P. Upadhyaya, H. Ganther, S. Vadhanavikit and H. Thompson, *Carcinogenesis*, 1994, **15**, 187–192.
8 S. Sugie, T. Tanaka and K. El-Bayoumy, *J. Health Sci.*, 2000, **46**, 422–425.
9 (*a*) K. El-Bayoumy, P. Upadhyaya, Y. H. Chae, O. S. Sohn, C. V. Rao, E. Fiala and B. S. Reddy, *J. Cell. Biochem.*, 1995, 92–100; (*b*) B. S. Reddy, S. Sugie, H. Maruyama, K. El-Bayoumy and P. Marra, *Cancer Res.*, 1987, **47**, 5901–5904.
10 (*a*) B. S. Reddy, A. Rivenson, K. El-Bayoumy, P. Upadhyaya, B. Pittman and C. V. Rao, *J. Natl. Cancer Inst.*, 1997, **89**, 506–512; (*b*) B. S. Reddy, A. Rivenson, N. Kulkarni, P. Upadhyaya and K. El-Bayoumy, *Cancer Res.*, 1992, **52**, 5635–5640.
11 (*a*) S. Ghosh, R. K. Das, A. Sengupta and S. Bhattacharya, *Biol. Trace Elem. Res.*, 2005, **105**, 171–185; (*b*) R. K. Das, S. K. U. Hossain and S. Bhattacharya, *Cancer Lett.*, 2005, **230**, 90–101.
12 S. S. Roy, P. Chakraborty, P. Ghosh, S. Ghosh, J. Biswas and S. Bhattacharya, *Redox Rep.*, 2012, **17**, 157–166.
13 P. Chakraborty, S. K. U. Hossain and S. Bhattacharya, *Cancer Chemother. Pharmacol.*, 2009, **64**, 971–980.
14 Y. F. Qi, X. Q. Fu, Z. G. Xiong, H. T. Zhang, S. M. Hill, B. G. Rowan and Y. Dong, *PLoS One*, 2012, **7**, e31539, DOI: 10.1371/journal.pone.0031539.
15 (*a*) W. A. Mónica Álvarez-Pérez, M. A. Marć, J. Handzlik and E. Domínguez-Álvarez, *Molecules*, 2018, **23**, 628–647; (*b*) D. Bhattacherjee, C. Basu, Q. Bhardwaj, S. Mal, S. Sahu, R. Sur and K. P. Bhabak, *ChemistrySelect*, 2017, **2**, 7399–7406.
16 D. Plano, D. N. Karelia, M. K. Pandey, J. E. Spallholz, S. Amin and A. K. Sharma, *J. Med. Chem.*, 2016, **59**, 1946–1959.
17 Y. W. Liang, Y. L. Zhou, S. L. Deng and T. F. Chen, *ChemMedChem*, 2016, **11**, 2339–2346.
18 (*a*) Y. Anan, M. Kimura, M. Hayashi, R. Koike and Y. Ogra, *Chem. Res. Toxicol.*, 2015, **28**, 1803–1814; (*b*) K. El-Bayoumy, P. Upadhyaya, O. S. Sohn, J. G. Rosa and E. S. Fiala, *Carcinogenesis*, 1998, **19**, 1603–1607.
19 K. El-Bayoumy and R. Sinha, *Mutat. Res.-Fund. Mol. Med.*, 2004, **551**, 181–197.
20 L. A. Jacob, B. Matos, C. Mostafa, J. Rodriguez and J. K. Tillotson, *Molecules*, 2004, **9**, 622–626.
21 S. Saglam, A. Disli, Y. Erdogdu, M. K. Marchewka, N. Kanagathara, B. Bay and M. T. Gulluoglu, *Spectrochim. Acta, Part A*, 2015, **135**, 1011–1018.
22 D. Plano, Y. Baquedano, E. Ibanez, I. Jimenez, J. A. Palop, J. E. Spallholz and C. Sanmartin, *Molecules*, 2010, **15**, 7292–7312.
23 J. C. Yarrow, Z. E. Perlman, N. J. Westwood and T. J. Mitchison, *BMC Biotechnol.*, 2004, **4**, 21, DOI: 10.1186/1472-6750-4-2.
24 (*a*) G. Mugesh, W. W. du Mont and H. Sies, *Chem. Rev.*, 2001, **101**, 2125–2179; (*b*) K. P. Bhabak and G. Mugesh, *Acc. Chem. Res.*, 2010, **43**, 1408–1419.
25 K. P. Bhabak and G. Mugesh, *Chem. – Eur. J.*, 2007, **13**, 4594–4601.
26 C. Szabo, H. Ischiropoulos and R. Radi, *Nat. Rev. Drug Discovery*, 2007, **6**, 662–680.
27 (*a*) K. P. Bhabak and G. Mugesh, *Chem. – Eur. J.*, 2010, **16**, 1175–1185; (*b*) K. P. Bhabak, K. Satheeshkumar, S. Jayavelu and G. Mugesh, *Org. Biomol. Chem.*, 2011, **9**, 7343–7350; (*c*) K. P. Bhabak, A. A. Vernekar, S. R. Jakka, G. Roy and G. Mugesh, *Org. Biomol. Chem.*, 2011, **9**, 5193–5200.
28 M. Anjomshoa, S. J. Fatemi, M. Torkzadeh-Mahani and H. Hadadzadeh, *Spectrochim. Acta, Part A*, 2014, **127**, 511–520.
29 S. K. Ghosh, S. K. U. Hossain, S. Bhattacharya and S. C. Bhattacharya, *J. Photochem. Photobiol., B*, 2005, **81**, 121–128.
30 S. L. Deng, D. L. Zeng, Y. Luo, J. F. Zhao, X. L. Li, Z. N. Zhao and T. F. Chen, *RSC Adv.*, 2017, **7**, 16721–16729.
31 (*a*) C. Bocca, F. Bozzo and A. Miglietta, *Anticancer Res.*, 2014, **34**, 1793–1800; (*b*) C. Bocca, M. Ievolella, R. Autelli, M. Motta, L. Mosso, B. Torchio, F. Bozzo, S. Cannito, C. Paternostro, S. Colombatto, M. Parola and A. Miglietta, *Expert Opin. Ther. Targets*, 2014, **18**, 121–135; (*c*) K. M. W. Rahman, Y. W. Li, Z. W. Wang, S. H. Sarkar and F. H. Sarkar, *Cancer Res.*, 2006, **66**, 4952–4960.
32 T. Boopalan, A. Arumugam, C. Damodaran and L. Rajkumar, *Anticancer Res.*, 2012, **32**, 2801–2806.
33 G. M. Morris, D. S. Goodsell, R. S. Halliday, R. Huey, W. E. Hart, R. K. Belew and A. J. Olson, *J. Comput. Chem.*, 1998, **19**, 1639–1662.

